

#### How to cite this article:

Tonso VM, Yamauchi FI, Mussi TC, Figueiredo E, Baroni RH. Comparative study between monoexponential and biexponential diffusion weighted imaging sequences in multiparametric prostate magnetic resonance imaging. *einstein* (São Paulo). 2019;17(3):eAO4615. [http://dx.doi.org/10.31744/einstein\\_journal/2019AO4615](http://dx.doi.org/10.31744/einstein_journal/2019AO4615)

#### Corresponding author:

Victor Martins Tonso  
Radiology Department  
Avenida Albert Einstein, 627/701, 4<sup>o</sup> floor,  
building D – Morumbi  
Zip code: 05652-900 – São Paulo, SP, Brazil  
Phone: (55 11) 2151-2452  
E-mail: victor.tonso@einstein.br

#### Received on:

June 1, 2018

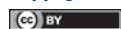
#### Accepted on:

Jan 21, 2019

#### Conflict of interest:

none.

#### Copyright 2019



This content is licensed under a Creative Commons Attribution 4.0 International License.

## ORIGINAL ARTICLE

# Comparative study between monoexponential and biexponential diffusion weighted imaging sequences in multiparametric prostate magnetic resonance imaging

Estudo comparativo entre as sequências de difusão monoexponencial e biexponencial na ressonância magnética multiparamétrica da próstata

Victor Martins Tonso<sup>1</sup>, Fernando Ide Yamauchi<sup>1</sup>, Thais Caldara Mussi<sup>1</sup>, Eduardo Figueiredo<sup>2</sup>, Ronaldo Hueb Baroni<sup>1</sup>

<sup>1</sup> Hospital Israelita Albert Einstein, São Paulo, SP, Brazil.

<sup>2</sup> General Electric's Health Care, São Paulo, SP, Brazil.

DOI: [10.31744/einstein\\_journal/2019AO4615](https://doi.org/10.31744/einstein_journal/2019AO4615)

## ABSTRACT

**Objective:** To compare qualitatively and quantitatively, in terms of image quality, a new biexponential diffusion sequence protocol with the standard monoexponential diffusion protocol on multiparametric prostate magnetic resonance imaging. **Methods:** This study had a prospective data collection and cross-sectional analysis. Between August and November 2017, a total of 70 patients who underwent multiparametric prostate magnetic resonance imaging due to clinical suspicion of prostatic neoplasia were recruited. The images obtained were evaluated by two independent readers regarding subjective/qualitative criteria (six criteria) and objective/quantitative criteria (three criteria), always comparing the monoexponential to biexponential acquisition protocols. The results were compared by statistical analysis (interobserver agreement – Gwet coefficient; analysis of the qualitative variables – Stuart-Maxwell test; and analysis of the quantitative variables – Wilcoxon test). **Results:** After exclusion of four patients, the final sample consisted of 66 patients. A good/excellent inter observer agreement was established for subjective criteria (except in one criteria). For the qualitative analysis the amount of good or excellent evaluations was higher for the monoexponential protocol (except in one category), with evidence of significant differences for three criteria (diffusion weighted imaging global quality; diffusion weighted imaging signal-to-noise ratio; and apparent diffusion coefficient signal-to-noise ratio). For the quantitative data analysis, the monoexponential protocol showed less variability of the anteroposterior diameters, meaning less distortion of the images, and better estimated signal-to-noise ratio. **Conclusion:** In our data, the quality of the images of the monoexponential standard diffusion sequence was qualitatively and quantitatively superior to those of the biexponential diffusion weighted imaging sequence.

**Keywords:** Magnetic resonance imaging; Diffusion magnetic resonance imaging; Multiparametric prostate magnetic resonance imaging; Monoexponential diffusion; Biexponential diffusion; Intravoxel incoherent motion; Prostatic neoplasms

## RESUMO

**Objetivo:** Comparar qualitativa e quantitativamente, em termos de qualidade de imagem, um novo protocolo de sequência de difusão biexponencial com o protocolo de difusão monoexponencial padrão,

em ressonância magnética multiparamétrica da próstata. **Métodos:** Estudo com coleta prospectiva e análise transversal. Entre agosto e novembro de 2017, foram recrutados 70 pacientes que realizaram ressonância magnética multiparamétrica da próstata, por suspeita de neoplasia prostática. As imagens obtidas por ambas as sequências foram avaliadas por dois leitores independentes, quanto a critérios de avaliação subjetiva/qualitativa (seis critérios) e objetiva/quantitativa (três critérios), sempre comparando os protocolos de aquisição monoexponencial e biexponencial. Os resultados foram comparados por análise estatística (concordância interobservador – coeficiente de Gwet; análise das variáveis qualitativas – teste de Stuart-Maxwell; e análise das variáveis quantitativas – testes de Wilcoxon). **Resultados:** Após exclusão de quatro pacientes, a amostra final foi composta por 66 pacientes. Uma boa/excelente concordância interobservador foi estabelecida para critérios subjetivos (exceto em um critério). Para a análise qualitativa, a quantidade de avaliações boas ou excelentes foi maior para o protocolo monoexponencial (exceto em uma categoria), com evidências de diferenças significativas para três critérios (qualidade global da imagem ponderada em difusão, relação sinal-ruído na imagem ponderada em difusão e relação sinal-ruído ADC). Para a análise quantitativa dos dados, o protocolo monoexponencial apresentou menor variabilidade dos diâmetros anteroposteriores, o que significou menos distorção das imagens, e melhor relação sinal-ruído estimada. **Conclusão:** Em nossos dados, a qualidade das imagens da sequência de difusão padrão monoexponencial foi qualitativa e quantitativamente superior àquelas da sequência teste biexponencial.

**Descritores:** Imagem por ressonância magnética; Imagem de difusão por ressonância magnética; Ressonância magnética multiparamétrica da próstata; Difusão monoexponencial; Difusão biexponencial; Movimento incoerente intravoxel; Neoplasias da próstata

## INTRODUCTION

Prostate cancer (PCa) is the most common tumor in men, except for non-melanoma skin tumors, and the second leading cause of death in this population.<sup>(1)</sup> Adenocarcinoma is the most frequent histological subtype responsible for 95% of prostate tumors, and early detection has a key role in the management and can substantially alter the disease prognosis.<sup>(2-5)</sup> Multiparametric prostate magnetic resonance imaging (mpMRI) plays an increasingly important role at this scenario.

Currently, the guidelines of the largest urology societies still recommend screening with prostate-specific antigen (PSA) and digital rectal examination.<sup>(6,7)</sup> If one or both are altered, a random ultrasound guided prostate biopsy follows as a general strategy for PCa detection. On the other hand, in the clinical practice of urologist, mpMRI is already largely used before the biopsy to precisely stratify the lesion and guide the biopsy, preferably with a fusion imaging guided biopsy procedure. This strategy allows a better chance to correctly sample the index lesion, reducing overdiagnosis of non-clinically significant lesions.

Diffusion weighted imaging (DWI) has been shown to be an essential component in the routine mpMRI examination protocol.<sup>(4,8-10)</sup> Conventional DWI is based on a simplified monoexponential mathematical diffusion model that enables the evaluation of molecular diffusion of water in tissue. It consists of a fast component that reflects the perfusion, in theory ultimately reflecting the irrigation of a given tissue, and a slow component that reflects diffusion.<sup>(11)</sup> The fast decay occurs at low b values, therefore it is necessary to sample the images with multiple b values in a range below 200s/mm<sup>2</sup>.

In 1988, Le Bihan et al., first described the diffusion technique based on a biexponential DWI model rather than a monoexponential model, also called “intravoxel incoherent motion” (IVIM).<sup>(12)</sup> In this biexponential model, biological tissues contain two distinct environments: molecular diffusion of water (true diffusion) and microcirculation of blood in the capillary network (perfusion). This concept has the advantage of accurately measuring the diffusion component (true diffusion), and additionally analyze the perfusion component, indirectly evaluating the capillary vascularization of a given tissue or lesion. It basically consists of acquiring diffusion weighted imaging with multiple b values to estimate the diffusion and perfusion parameters.

In sum, the biexponential DWI/IVIM model has the ability of gathering tissue perfusion information by separately evaluating perfusion and diffusion components, without using intravascular contrast media, which may promote increased detection with a better characterization of PCa, ultimately increasing the accuracy of the method.

A problem that limits the clinical applicability of the method is that current studies addressing this matter show high heterogeneity between acquisition protocols, with discordant or non-reproducible results.<sup>(13-16)</sup> This is a critical point of the technique and may be a barrier to its potential clinical use: there is no well-established or accepted protocol that is replicable in different organizations. In order to address this limitation, we designed a feasible and reproducible biexponential diffusion protocol, which includes well-established parameters used in conventional DWI for the true diffusion part, besides multiple b values in the lower range for appropriate perfusion component estimation.

## OBJECTIVE

To qualitatively and quantitatively compare the image quality of a biexponential diffusion sequence protocol

with the standard monoexponential diffusion protocol on multiparametric prostate magnetic resonance imaging.

## METHODS

### Population and ethical aspects

Seventy patients were recruited between August 2017 and November 2017 to be included in this prospective study approved by the Ethics Committee under protocol 996.878, CAAE: 30407914.3.0000.0071. They underwent mpMRI without an endorectal coil, solely and exclusively for clinical indications. The inclusion criteria were clinical suspicion of a clinically significant prostate tumor, increased levels of PSA and/or altered rectal touch. Exclusion criteria were contraindications to the method (use of devices not compatible with MRI, claustrophobia, among others), technical problems in the acquisition or post-processing of images and analysis by only one reader.

### Magnetic resonance imaging protocol

Patients underwent routine prostate mpMRI at 3 Tesla machine (Discovery MR750w, GE Healthcare, Milwaukee, USA), which also included a conventional monoexponential DWI sequence. A modified DWI sequence was added to the acquisition protocol (biexponential DWI sequence), including additional b acquisitions and making the sequence suitable for latter biexponential IVIM fitting (Figure 1) – full protocols in annex 1. The images were acquired using a surface coil. The total acquisition time of the biexponential DWI sequence was 8 minutes and 12 seconds.

## Methods of analysis

### Qualitative component

The images were read by two radiologists with more than 5 years experience in mpMR, always comparing the images with the highest b values of each sequence and their respective apparent diffusion coefficient (ADC) maps, based on the following criteria: overall quality, signal-to-noise ratio, contrast resolution/zonal anatomy definition, lesion *versus* background definition, prostatic contours definition, image distortion and artifacts. A total of 14 rating criteria for each sequence were established (7 DWI criteria and 7 ADC criteria for both standard monoexponential and biexponential sequences). These criteria were judged according to the following scale: 1: very bad; 2: bad; 3: moderate; 4: good; and 5: excellent.<sup>(17)</sup>

### Quantitative component

Measurements were taken to quantitatively assess the presence and grade of image distortion and to evaluate the signal-to-noise ratio. To evaluate the degree of image distortion, the largest anteroposterior and laterolateral diameters of the prostate were measured in the T2 axial sequences (Figure 2), monoexponential diffusion and biexponential IVIM diffusion. The T2-weighted images served as references for the measurements of anteroposterior and laterolateral diameters, since they are less susceptible to distortions than the DWI images, which are based on echo planar imaging sequences, highly susceptible for distortions.

The signal-to-noise ratio of MRI is traditionally obtained by comparing the signal of a given tissue with the air signal (in theory, zero).<sup>(18)</sup> However, this is not possible in most prostate exams, including both diffusion sequences, since the small field of view (FOV) does not

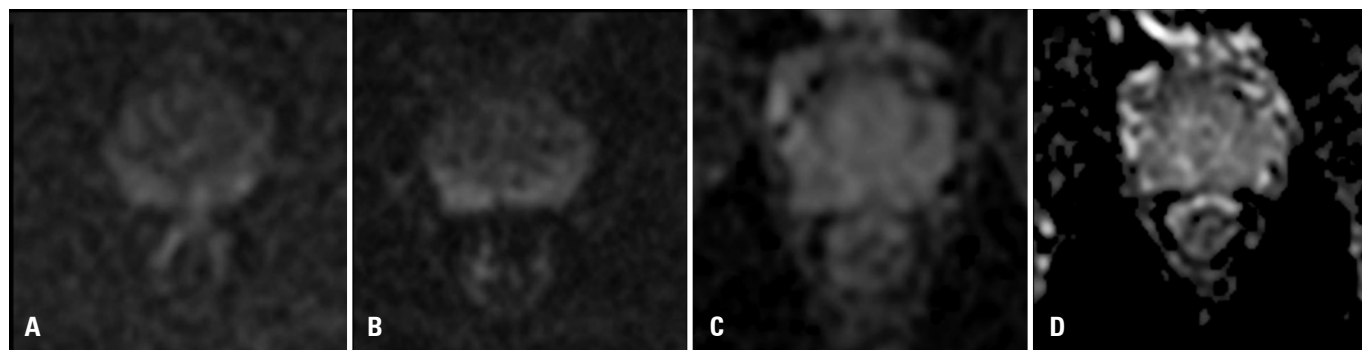


**Figure 1.** Standard monoexponential diffusion weighted imaging (A) and biexponential diffusion weighted imaging (B), with its respective apparent diffusion coefficient maps (C e D)

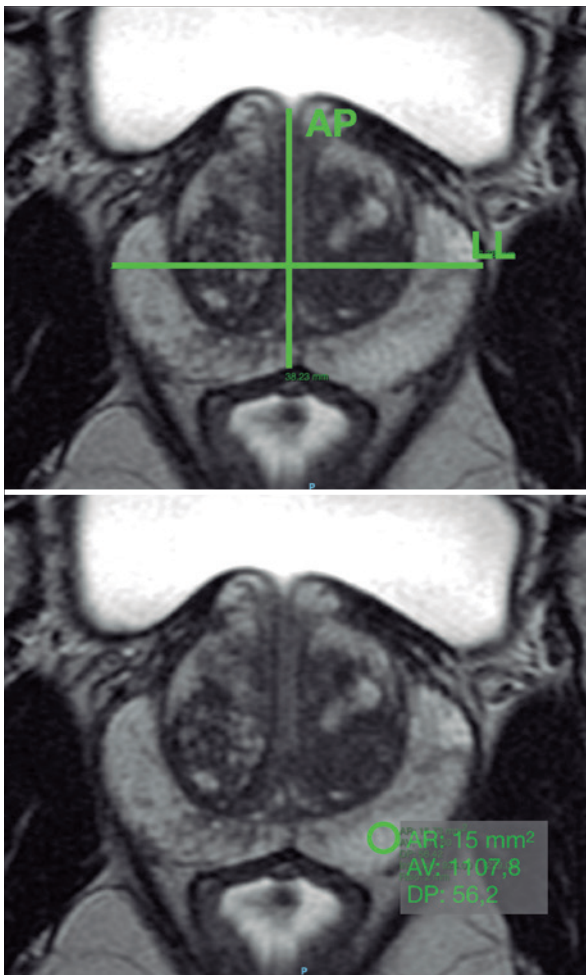


**Figure 2.** Anteroposterior and laterolateral diameters and example of region of interest positioning to obtain the signal-to-noise ratio

include air; hence, it is not possible to establish such ratio. The adopted alternative was to use the estimated signal-to-noise ratio (eSNR), which consists of a relation between the mean and the standard deviation of the signal intensity of the voxels of each sequence.<sup>(19,20)</sup> For this purpose, regions of interest (ROI) were positioned in peripheral zone (with a standard area of 15.3mm<sup>2</sup> and mean of 14.3mm<sup>2</sup>, varying from 5.5 to 15.3mm<sup>2</sup>), respecting the following methodology: positioned from T2 axial images in relatively little altered regions (Figure 2), always avoiding focal lesions, and replicated identically (same area and location) for the standard diffusion and biexponential sequence, and their respective ADC maps. This ROI area was arbitrarily established so that all positioning criteria cited above were met. The eSNR was calculated with the values obtained from the ADC maps.

### Statistical analysis

Following the methodology used, the statistical analysis was also divided into two groups, in order to separately evaluate the qualitative and quantitative components. As a first step, we evaluated the interobserver agreement using the Gwet coefficient. Once a satisfactory agreement between the two readers was achieved, the data of one of them was analyzed using the Stuart-Maxwell test for marginal homogeneity (or generalized McNemar test).<sup>(21,22)</sup>

The quantitative analyses, based on comparisons between the biexponential and monoexponential sequences for the quantitative variables (eSNR and diameters variation), were performed by Wilcoxon test for paired samples, considering a significance level of  $p < 0.05$ .

## RESULTS

Of the 70 patients initially included, 2 were excluded by artifacts related to image acquisition (magnetic susceptibility artifacts that degraded equally both diffusion sequences) and 2 by technical issues related to post-processing pipeline (software or dedicated workstation errors in the calculation of eSNR), and therefore the final sample consisted of 66 patients.

### Interobserver agreement

Interobserver agreement in our sample was good or excellent across all analyses, ranging from 0.62 to 0.95, except for a single item (“ADC signal-to-noise ratio” that had reasonable agreement among observers, 0.32).

### Qualitative component

For all evaluated criteria, except one of them (prostatic contours definition), good or excellent quality classification was always higher for the monoexponential sequence.

However, evidence of statistically significant differences was observed in only three categories: overall quality DWI, signal-to-noise ratio DWI and signal-to-noise ratio ADC (Table 1).

For four criteria (lesion *versus* background definition DWI, image distortion DWI, overall quality ADC and lesion *versus* background definition ADC), it was not possible to test hypotheses because there was a disparity/non-pairing of categories – a fundamental condition for analysis by the employed method in which categories needed to be paired. This occurred because only the biexponential sequence was evaluated as bad/very bad, generating this discrepancy with the monoexponential sequence that has always been evaluated as moderate or good/excellent in these questions.

**Table 1.** Comparisons between biexponential and monoexponential sequences regarding qualitative variables

Qualitative evaluation criteria	Biexponential	Monoexponential	p value
<b>Reader 1, DWI</b>			
Overall quality			0.046
Bad/very bad	0 (0.0)	0 (0)	
Moderate	8 (12.1)	4 (6.1)	
Good/excellent	58 (87.9)	62 (93.9)	
Signal-to-noise ratio			0.013
Bad/very bad	0 (0)	0 (0)	
Moderate	15 (22.7)	6 (9.1)	
Good/excellent	51 (77.3)	60 (90.9)	
Contrast resolution/zonal anatomy definition			0.059
Bad/very bad	0 (0)	0 (0)	
Moderate	10 (15.2)	5 (7.6)	
Good/excellent	56 (84.8)	61 (92.4)	
Lesion versus background definition			--
Do not apply	52 (78.8)	51 (77.3)	
Bad/very bad	1 (1.5)	0 (0)	
Moderate	8 (12.1)	3 (4.5)	
Good/excellent	5 (7.6)	12 (18.2)	
Prostatic contours definition			0.414
Bad/very bad	0 (0)	0 (0)	
Moderate	6 (9.1)	8 (12.1)	
Good/excellent	60 (90.9)	58 (87.9)	
Image distortion			--
Bad/very bad	2 (3.0)	0 (0)	
Moderate	9 (13.6)	10 (15.2)	
Good/excellent	55 (83.3)	56 (84.8)	
Artifacts			0.317
Bad/very bad	1 (1.5)	1 (1.5)	
Moderate	10 (15.2)	9 (13.6)	
Good/excellent	55 (83.3)	56 (84.8)	
<b>Reader 2, ADC</b>			
Overall quality			--
Bad/very bad	2 (3.0)	0 (0)	
Moderate	17 (25.8)	6 (9.1)	
Good/excellent	47 (71.2)	60 (90.9)	
Signal-to-noise ratio			<0.001
Bad/very bad	7 (10.6)	1 (1.5)	
Moderate	33 (50.0)	3 (4.5)	
Good/excellent	26 (39.4)	62 (93.9)	
Contrast resolution/zonal anatomy definition			0.292
Bad/very bad	2 (3.0)	1 (1.5)	
Moderate	19 (28.8)	13 (19.7)	
Good/excellent	45 (68.2)	52 (78.8)	
Lesion versus background definition			--
Do not apply	52 (78.8)	50 (75.8)	
Bad/very bad	1 (1.5)	0 (0)	
Moderate	4 (6.1)	4 (6.1)	
Good/excellent	9 (13.6)	12 (18.2)	

continue...

...Continuation

**Table 1.** Comparisons between biexponential and monoexponential sequences regarding qualitative variables

Qualitative evaluation criteria	Biexponential	Monoexponential	p value
<b>Prostatic contours definition</b>			
Bad/very bad	1 (1.5)	1 (1.5)	0.102
Moderate	9 (13.6)	5 (7.6)	
Good/excellent	56 (84.8)	60 (90.9)	
<b>Image distortion</b>			
Bad/very bad	2 (3.0)	1 (1.5)	0.050
Moderate	12 (18.2)	8 (12.1)	
Good/excellent	52 (78.8)	57 (86.4)	
<b>Artifacts</b>			
Bad/very bad	2 (3.0)	1 (1.5)	0.223
Moderate	8 (12.1)	7 (10.6)	
Good/excellent	56 (84.8)	58 (87.9)	
<b>Total</b>	<b>66 (100)</b>	<b>66 (100)</b>	

Results expressed as n (%). DWI: diffusion weighted imaging; ADC: apparent diffusion coefficient.

### Quantitative component: anteroposterior and laterolateral diameters

Anteroposterior diameters: monoexponential sequence presented smaller variation compared to the T2 sequence measurements (values ranging from -0.8 to +0.4), demonstrating lower image distortion in the anteroposterior axis, when compared to those measured within the bioexponential sequence, and it was statistically significant (p=0.009).

Laterolateral diameters: the biexponential sequence presented smaller variation with reference to the T2 sequence measurements (values ranging from -0.2 to +0.4), demonstrating lower image distortion in the laterolateral axis when compared to the monoexponential sequence, but it was not statistically significant (p=0.075) (Table 2).

**Table 2.** Comparison between biexponential and monoexponential regarding variation of anteroposterior and laterolateral diameters

Diameter	Differences in T2		p value
	biexponential-T2	monoexponential-T2	
Anteroposterior			0.009
Median (1 <sup>st</sup> quartile; 3 <sup>rd</sup> quartile)	0.00 (-0.20; 0.10)	-0.10 (-0.20; 0.00)	
Minimum; maximum	-1.00; 0.50	-0.80; 0.40	
Laterolateral			0.075
Median (1 <sup>st</sup> quartile; 3 <sup>rd</sup> quartile)	0.10 (0.00; 0.20)	0.10 (0.00; 0.20)	
Minimum; maximum	-0.20; 0.40	-0.50; 0.50	

## Quantitative component: estimated signal-to-noise ratio

The monoexponential sequence presented smaller spreading of the voxel signal intensity, demonstrating higher signal homogeneity and statistically significant eSNR ( $p < 0.001$ ) (Table 3).

**Table 3.** Comparison of biexponential and monoexponential sequences regarding estimated signal-to-noise ratio

eSNR	Biexponential	Monoexponential	p value
Standard deviation			<0.001
Median (1 <sup>st</sup> quartile-3 <sup>rd</sup> quartile)	113.0 (78.6-182.5)	79.8 (48.8111.8)	
Minimum-maximum	36.0-771.2	19.9381.9	

eSNR: estimated signal-to-noise ratio.

## DISCUSSION

In general, our data showed superior subjective/qualitative analysis criteria to the monoexponential standard compared to the biexponential sequence. This better evaluation is also reinforced by the four criteria, since it was not possible to perform the hypothesis test because only the biexponential IVIM sequence was evaluated as bad/very bad (the monoexponential sequence did not receive such a classification in any of the items). However, since this is a subjective analysis, one fact that may have influenced is familiarity of the readers with the standard sequence and a certain strangeness with the test sequence.

Analyzing the overall quality criteria (perhaps the most important question), we observe an interesting aspect. Specifically in the overall quality-DWI, there is a very similar distribution of evaluations, with only four divergent cases, and prevalence of good/excellent for both sequences, which shows that the test sequence is not so far from the standard sequence. However, when looking specifically to overall quality-ADC, we noted again the superiority of the standard sequence, with more cases evaluated with good/excellent for the monoexponential sequence, and only the biexponential sequence receiving poor/very poor evaluations. Eventually this fact can be explained by the multiple b values obtained in the biexponential protocol. As the ADC maps are obtained from the DWI images, and for the biexponential model it is necessary to obtain several b values at different times, the images are more susceptible to motion artifacts due to the presence/passage of gas through the rectum.

This first component of our results resembles in part those obtained in the recent work of Merisaari

et al.,<sup>(16)</sup> who also had as conceptual problem the lack of consensus regarding an ideal protocol for the use of the biexponential IVIM model. They tested four adjustment models for the IVIM and, additionally, four mathematical adjustment models for DWI, also always with superior results for the monoexponential model.

Regarding the quantitative parameters, once again monoexponential model showed superior results compared to biexponential IVIM model, with less image distortion in the anteroposterior axis and better eSNR. These results may, at least partly, be explained by the particularity of the multiple b values acquired in the IVIM protocol, making it more susceptible to motion, consequently with more image distortion and higher signal heterogeneity in the acquired images. This aspect could eventually be minimized only with an adjustment of the post-processing parameters. The MR scanners diffusion software, by default, uses all b values acquired to generate the ADC maps, but this can be customized by indicating how many and which b values should be used. This would potentially minimize the artifacts on the ADC biexponential IVIM maps, bringing it closer in quality to the ADC monoexponential maps. This possibility should be object of future work.

A positive aspect for the biexponential sequence in our results that should be emphasized is that, besides the superiority of the monoexponential diffusion protocol, the disparity between the numbers obtained was not so great; considering that it was a first adjustment attempt for the biexponential sequence, new efforts and improvements may make it better. Valerio et al.,<sup>(23)</sup> recently showed increased specificity and sensitivity in the detection of cancers in the peripheral zone using the biexponential IVIM model, a result that also encourages the continuous development of the sequence so that it can be incorporated into the mpMRI.

Considering the potential of the biexponential diffusion model to become a “one-stop-shop” sequence, *i.e.*, having the ability to – in a single acquisition – assess the true restriction component and tissue perfusion component, what potentially could make the use of paramagnetic contrast unnecessary, unburdening the method and consequently making it more accessible. Therefore, we believe that efforts should be made to improve this sequence in new studies.

Our study had some limitations. Despite having a prospective collection with cross-sectional analysis performed by two independent observers, they were not masked in relation to the nature of the sequences.

Masking was not possible due to the intrinsic peculiarity of the different b values of each acquisition technique (the monoexponential sequence is acquired with three b values and the biexponential with ten b values), an aspect easily perceived by the examiners. In addition, much of the results came from a subjective analysis, that is, dependent on the experience of the readers. Furthermore, image pattern of the new sequence may have caused some level of strangeness, since the monoexponential sequence is already part of the institutional protocol for some time, and readers are used to the image generated by this technique. Hence, it would not be possible to discard a familiarity bias. However, to minimize and normalize the subjective aspect, objective quantitative criteria were also evaluated, which were concordant with the subjective criteria.

In a future study, we aim to explore the additional diffusion metrics that biexponential model can provide, especially that pseudo-diffusion component, and its impact to lesion classification, which is a major advantage of the biexponential model, with potential to add diagnostic information to the evaluation of mpMRI.

## CONCLUSION

The quality of the images of the monoexponential standard diffusion sequence was qualitatively and quantitatively superior to those of the biexponential diffusion weighted imaging sequence.

## ACKNOWLEDGEMENTS

To the biomedical professional Joyce Prado de Oliveira, for commitment and willingness to help in the course of the project. To the engineer Eduardo Figueiredo, for support and suggestions given, and to GE HealthCare do Brasil, for the partnership in this project. To the biomedical, nurses, technicians and administrators of the Diagnostic Imaging Department of the *Hospital Albert Einstein*, always committed to obtaining the best exams. Elivane da Silva Victor, for assistance in statistical planning and analysis of this work.

## AUTHORS' INFORMATION

Tonso VM: <http://orcid.org/0000-0002-6362-3825>  
 Yamauchi FI: <http://orcid.org/0000-0002-4633-3711>  
 Mussi TC: <http://orcid.org/0000-0001-8231-2646>  
 Figueiredo E: <http://orcid.org/0000-0002-3440-0737>  
 Baroni RH: <http://orcid.org/0000-0001-8762-0875>

## REFERENCES

1. Instituto Nacional de Cancer (INCA). Estimativas para o ano de 2016 das taxas brutas de incidência por 100 mil habitantes e do número de casos novos de câncer, segundo sexo e localização primária [Internet]. Rio de Janeiro: INCA; c1996-2018 [citado 2018 Jan 15]. Disponível em: <https://www.inca.gov.br/numeros-de-cancer>
2. National Cancer Institute (NIH). Surveillance, Epidemiology, and End Results Program. Cancer Stat Facts: Prostate Cancer [Internet]. USA: NIH; s.d. [cited 2018 Jan 15]. Available from: <http://seer.cancer.gov/statfacts/html/prost.html>
3. Cancer Research UK. Prostate cancer survival statistics [Internet]. UK: Cancer Research UK; 2015 [cited 19 Oct 2016]. Available from: <http://www.cancerresearchuk.org/health-professional/cancer-statistics/statistics-by-cancer-type/prostate-cancer/survival>
4. Bonekamp D, Jacobs MA, El-Khouli R, Stoianovici D, Macura KJ. Advancements in MR imaging of the prostate: from diagnosis to interventions. *Radiographics*. 2011;31(3):677-703. Review.
5. Weissleder R, Wittenberg J, Harinsinghani M, Chen J. *Primer of diagnostic imaging*. 5th ed. St Louis: Mosby; 2011.
6. Schröder FH, Hugosson J, Roobol MJ, Tammela TL, Ciatto S, Nelen V, Kwiatkowski M, Lujan M, Lilja H, Zappa M, Denis LJ, Recker F, Berenguer A, Maattanen L, Bangma CH, Aus G, Villers A, Rebillaud X, van der Kwast T, Blijenberg BG, Moss SM, Koning HJ, Auvinen A; ERSPC Investigators. Screening and prostate-cancer mortality in a randomized European study. *N Engl J Med*. 2009;360(13):1320-8.
7. American Urological Association (AUA). Early detection of prostate cancer [Internet]. USA: AUA Guideline. Published 2013; Reviewed and Validity Confirmed 2015 [cited 2018 Jan 12]. Available from: [http://www.auanet.org/guidelines/early-detection-of-prostate-cancer-\(2013-reviewed-and-validity-confirmed-2015](http://www.auanet.org/guidelines/early-detection-of-prostate-cancer-(2013-reviewed-and-validity-confirmed-2015)
8. Bhavsar A, Verma S. Anatomic imaging of the prostate. *Biomed Res Int*. 2014;2014:728539. Review.
9. Mullins JK, Bonekamp D, Landis P, Begum H, Partin AW, Epstein JI, et al. Multiparametric magnetic resonance imaging findings in men with low-risk prostate cancer followed using active surveillance. *BJU Int*. 2013; 111(7):1037-45.
10. Rais-Bahrami S, Siddiqui MM, Vourganti S, Turkbey B, Rastinehad AR, Stamatakis L, et al. Diagnostic value of biparametric magnetic resonance imaging (MRI) as an adjunct to prostate-specific antigen PSA-based detection of prostate cancer in men without prior biopsies. *BJU Int*. 2015;115(3):381-8.
11. Bammer R. Basic principles of diffusion-weighted imaging. *Eur J Radiol*. 2003;45(3):169-84. Review.
12. Le Bihan D, Breton E, Lallemand D, Aubin ML, Vignaud J, Laval-Jeantet M. Separation of diffusion and perfusion in intravoxel incoherent motion MR imaging. *Radiology*. 1988;168(2):497-505.
13. Koh DM, Collins DJ, Orton MR. Intravoxel incoherent motion in body diffusion-weighted MRI: reality and challenges. *AJR Am J Roentgenol*. 2011; 196(6):1351-61. Review.
14. Koh DM, Blackledge M, Collins DJ, Padhani AR, Wallace T, Wilton B, et al. Reproducibility and changes in the apparent diffusion coefficients of solid tumours treated with combretastatin A4 phosphate and bevacizumab in a two-centre phase I clinical trial. *Eur Radiol*. 2009;19(11):2728-38.
15. Lecler A, Savatovsky J, Balvay D, Zmuda M, Sadik JC, Galatoire O, et al. Repeatability of apparent diffusion coefficient and intravoxel incoherent motion parameters at 3.0 Tesla in orbital lesions. *Eur Radiol*. 2017;27(12):5094-103.
16. Merisaari H, Movahedi P, Perez IM, Toivonen J, Pesola M, Taimen P, et al. Fitting methods for intravoxel incoherent motion imaging of prostate cancer on region of interest level: repeatability and gleason score prediction. *Magn Reson Med*. 2017;77(3):1249-64.

17. Likert R. A Technique for the Measurement of Attitudes. New York: The Science Press; 1932. [Archives of Psychology, nº 140].
18. Sijbers P, Scheunders P, Bonnet N, Van Dyck D, Raman E. Quantification and improvement of the signal-to-noise ratio in a magnetic resonance image acquisition procedure. Magn Reson Imaging. 1996;14(10):1157-63.
19. Heverhagen JT. Noise measurement and estimation in MR imaging experiments. Radiology. 2007;245(3):638-9.
20. Rosenkrantz AB, Chandarana H, Pfeuffer J, Triolo MJ, Shaikh MB, Mossa DJ, et al. Zoomed echo-planar imaging using parallel transmission: impact on image quality of diffusion-weighted imaging of the prostate at 3T. Abdom Imaging. 2015;40(1):120-6.
21. Altman DG. Practical statistics for medical research. London: CRC Press; 1990.
22. Liu JP, Hsueh HM, Hsieh E, Chen JJ. Tests for equivalence or non-inferiority for paired binary data. Statist Med. 2002;21(2):231-45.
23. Valerio M, Zini C, Fierro D, Giura F, Colarieti A, Giuliani A, et al. 3T multiparametric MRI of the prostate: does intravoxel incoherent motion diffusion imaging have a role in the detection and stratification of prostate cancer in the peripheral zone? Eur J Radiol. 2016;85(4):790-4.

#### Annex 1. Diffusion protocols

Parameters	Values	
	Biexponential protocol	Monoexponential protocol
Machine	3.0 Tesla (Discovery MR 750w, GE Healthcare)	3.0 Tesla (Discovery MR 750w, GE Healthcare)
Pulse sequence	DWI single-shot spin-echo	DWI single-shot spin-echo
Scan plan	oblique	oblique
Acquisition type	2D	2D
Breath	Free	Free
TR/TE	4686/255 ~ 67.5 (optimized to the TR)	4686/255 ~ 67.5 (optimized to the TR)
Slice thickness, mm	3	3
Spacing	0	0
Number of slices	16	24
Sweep coverage	48mm	72mm
Matrix	120 × 120	120 × 120
FOV, mm	200	200
Phase encode direction	A/P	A/P
Number of medians	Variable	Variable
Sensitive encoding factor	Parallel acquisition with auto-generalized auto-calibration	Parallel acquisition with auto-generalized auto-calibration
B values (s/mm <sup>2</sup> ) and number of excitations	0 (2), 10 (2), 30 (2), 50, (2), 80 (2), 100 (2), 200 (2), 400 (4) e 1000 (8)	50 (12), 1000 (16)
Receiver bandwidth, Hz/pixel	+/-250	+/-250
Fat suppression	FOCUS	FOCUS
Acquisition time	8 minutes and 12 seconds	5 minutes and 53 seconds

FOV: filed-of-field; FOCUS: field-of-view optimized and constrained undistorted single shot; TR/TE: repetition time/echo time.